PROFESSOR J. SIMMER (Orcid ID : 0000-0002-7192-6105)

Article type : Original Paper

Characteristics of the Transverse 2D Uniserial Arrangement of Rows of Decussating Enamel Rods in the Inner Enamel Layer of Mouse Mandibular Incisors

Charles E. Smith[1,2], Yuanyuan Hu[1], Jan C-C. Hu[1] and James P. Simmer[1]

[1]Department of Biologic and Materials Sciences, University of Michigan School of Dentistry, 1210 Eisenhower Place, Ann Arbor, Michigan USA 48108

[2]Department of Anatomy & Cell Biology, Faculty of Medicine, McGill University, 3640 University Street, Montreal, QC CANADA H3A 0C7

Charles E. Smith: charles.smith@mcgill.ca, +1-514-398 4520

Yuanyuan Hu: yyhu@umich.edu, +1-734-975 9326

Jan C-C Hu: janhu@umich.edu, +1-734-763 6769

James P. Simmer: jsimmer@umich.edu, +1-734-764 4676

Corresponding Author: James P. Simmer: jsimmer@umich.edu, +1-734-764-4676

Keywords: Enamel formation, rows of enamel rods, spatial distribution, decussation, row irregularities, ameloblast movement

Word Count: Abstract: 457 words Main Text: 7878 words

Running Title: 2D Organization of Rows of Enamel Rods in Mouse Mandibular Incisors

Abstract

The 2D arrangement of rows of enamel rods with alternating (decussating) tilt angles across the thickness of the inner layer in rat and mouse incisor enamel is well known and assumed to occur in a uniform and repetitive pattern. Some irregularities in the arrangement of rows have been reported but no detailed investigation of row structure across the entire inner enamel layer currently exists. This investigation was undertaken to determine if the global row pattern in mouse mandibular incisor enamel is predominately regular in nature with only occasional anomalies or if rows of enamel rods have more spatial complexity than previously suspected. The data from this investigation indicate that rows of enamel rods are highly variable in length and have complex transverse arrangements across the width and thickness of the inner enamel layer. The majority of rows are short or medium in length, with 87% having <100 rods per row). The remaining 13% are long rows (with 100-233 rods per row) that contain 46% of all enamel rods seen in transverse sections. Variable numbers of rows were associated with the lateral, central and mesial regions of the enamel layer. Each region contained different ratios of short medium and long rows. A variety of relationships were found along the transverse length of rows in each region, including uniform associations of alternating rod tilts between neighboring rows, and instances where two rows having the same rod tilt were paired for variable distances then moved apart to accommodate rows of opposite tilt. Sometimes a row appeared to branch into two rows with the same tilt, or conversely where two rows merged into one row depending upon the mesial-to-lateral direction in which the row was viewed. Some rows showed both pairing and branching/merging along their length. These tended to be among the longest rows identified, and they often crossed the central region with extensions into the lateral and mesial regions. The most frequent row arrangement was a row of petite length nestled at the side of another row having the same rod tilt (30% of all rows). These were termed “focal stacks” and may relate to the evolution of uniserial rat and mouse incisor enamel from a multilayered ancestor. The mesial and lateral endpoints of rows also showed complex arrangements with the dentinoenamel junction (DEJ), the inner enamel layer itself, and the boundary area to the outer enamel layer. It was concluded that the diversity in row lengths and various spatial arrangements both within and between rows across the transverse plane provides a method to interlock

the enamel layer across each region and keep the enamel layer compact relative to the curving DEJ surface. The uniserial pattern for rows in mouse mandibular incisors is not uniform but diverse and very complex.

Introduction

There has been considerable interest over the past century and a half in classifying the many shapes and arrangements of enamel rods present in the teeth of extinct and extant mammals, especially rodents (Tomes, 1850, Kawai, 1955, von Koenigswald, 1985, Sahni, 1985, Martin, 1999, Martin, 2007). The diversity of enamel rod forms and organizational patterns, referred to as the enamel "Schmelzmuster" in the paleontological literature, e.g., (von Koenigswald and Clemens, 1992, Yilmaz et al., 2015), has led many investigators to suspect that most if not all the different patterns described correlate to differences in diet and a natural driving force directed toward developing the enamel layer with efficient and effective abrasion and fracture resistance (von Koenigswald, 1985, von Koenigswald et al., 1987, Vieytes et al., 2007, Yahyazadehfar et al., 2013). Other investigators have used rod organizational patterns to help define possible evolutionary interrelationships among predecessors across specific mammalian orders, e.g., (Kawai, 1955, Sahni, 1985, von Koenigswald, 1985, Martin, 1993, Martin, 1999, Martin, 2007 , Stefen and Rensberger, 1999, Tabuce et al., 2007, von Koenigswald et al., 2011, Alloing-Séguier et al., 2014). In the past half century, the shape and arrangement of enamel rods have also been of special interest as potential indicators of the pathways ameloblasts follow in secreting the enamel layer (Boyde, 1969, Osborn, 1970, Warshawsky, 1978, Risnes, 1979a, Radlanski and Renz, 2006, Hanaizumi et al., 2010, Cox, 2013, Alloing-Séguier et al., 2017, Alloing-Seguier et al., 2018).

Diversity of rod shapes and organizational patterns in mammalian enamel occurs not only on different sides of the same tooth but also between different tooth types in the same mammal as well as dramatically between different mammalian species (Boyde, 1969, Risnes, 1979b, von Koenigswald and Clemens, 1992, Moinichen et al., 1996, Lyngstadaas et al., 1998, Goldberg et al., 2014). Underneath all this diversity, there are certain structural fundamentals shared by enamel covering all extant mammalian teeth. For example, the elemental building blocks of mammalian enamel are small but elongated crystallites of carbonated hydroxyapatite either grouped together into much larger enamel rods (prisms) or filling the spaces between the rods (interrod/interprismatic) (Boyde, 1969, von Koenigswald and Clemens, 1992, Yilmaz et al., 2015). Enamel rods originate near the dentinoenamel junction (DEJ) and travel toward the outer surface of the enamel layer, usually along some nonlinear path that may follow an angularly segmented, sigmoid or wavy/spiral trajectory (Boyde, 1969, Warshawsky, 1971, Warshawsky, 1978, Sahni, 1985, von Koenigswald and Clemens, 1992, Alloing-

Séguier et al., 2017, Alloing-Seguier et al., 2018). Enamel rods traverse the thickness of the enamel layer usually in groups that follow the same nonlinear path (Alloing-Séguier et al., 2017, Alloing-Seguier et al., 2018). Immediately adjacent groups of enamel rods follow different nonlinear paths, often at an opposite angle relative to neighboring groups of rods. This creates arrangements in the deeper regions of the enamel layer called Hunter-Schreger bands, a term that has come to imply sites within an enamel layer of a mammal tooth where groups of enamel rods decussate, that is, change angles relative to each other (Boyde, 1969, Hanaizumi et al., 1996, Hanaizumi et al., 2010, Kawai, 1955, Sahni, 1985, von Koenigswald, 1985, von Koenigswald and Pfretzschner, 1987, Osborn, 1990, Stefen and Rensberger, 1999, Tabuce et al., 2007, Lynch et al., 2010, von Koenigswald et al., 2011, Alloing-Séguier et al., 2017). In rat and mouse incisors, Hunter-Schreger bands are not prominent and are superseded by an arrangement where the grouping of enamel rods occurs in single rows filling the inner region of the enamel layer. Each successive row characteristically is arrayed at an angle opposite to the row above and below across the thickness of the inner enamel layer (Tomes, 1850, Sahni, 1985, von Koenigswald, 1985, Martin, 1993). In longitudinal sections of rat and mouse incisor enamel, this gives rise to the classical appearance of side-by-side lamellar sheets of vertically stacked rows arrayed at sequentially alternating angles with an incisal slant along the length and thickness of the inner enamel layer (Boyde, 1969, Warshawsky, 1971, Risnes, 1979b).

There have been controversies about rod arrangement in ancestral rat and mouse incisor enamel (pauciserial versus multiserial), but for the most part paleontologists agree that the enamel in these mammals originated as a double layered structure with decussating portions of enamel rods forming the inner layer (portio interna) and radial portions of rods (traveling parallel to one another in straight lines) forming an outer layer (portio externa) (Tomes, 1850, Sahni, 1985, von Koenigswald, 1985, Martin, 1993). The inner layer was multilayered in arrangement, that is, with several rows of rods stacked on top of each other all having the same tilt angle, followed by several rows of rods having an opposite tilt angle, repeated across the thickness of the inner enamel layer. Over time this arrangement evolved into the classic uniserial pattern of single alternating rows present in modern rat and mouse incisor enamel (Sahni, 1985, von Koenigswald, 1985, Martin, 1993).

Most descriptions of the uniserial pattern of rods in mouse and rat incisor enamel have implied it is uniform in arrangement and has a highly repetitive alternation of tilt angles between rows across the thickness of the inner enamel layer (Sahni, 1985, von Koenigswald, 1985, Martin, 1993). Risnes (1979b) noted oddities in rodent enamel uniserial patterns and he described instances where at least 6 different types of irregularities (aberrations) in row organization could be identified within the inner

enamel layer of rat incisor enamel. These included (1) rows having shorter length than its neighbors, (2) deviations in the transverse orientation of rows especially near the mesial and lateral sides of the enamel layer, (3) fusing or bifurcation in some rows depending upon the direction of view along the row, (4) parallel rather than opposing rod angulations between some neighboring rows, (5) directional changes by some rods out of original row orientation, and (6) variations in the dimensions of profile outlines of some rods. The author further noted that these aberrations seemed plentiful, but he did not quantify their frequencies and was unable to reach any specific conclusions about the significance of these irregularities to structural integrity within the inner enamel layer. There was speculation that these irregularities may have something to do with alterations in spatial packing within the ameloblast layer as the rods were being formed. This author also noted in a later study that similar irregularities in row structure were also present in mouse incisor enamel (Moinichen et al., 1996). These observations about peculiarities in uniserial row arrangements in rat and mouse incisor enamel seem to have received little attention/interest and there have been no subsequent studies probing this issue in more detail.

In a recent study on the gross distribution of enamel rods within transverse (cross) sections of mouse mandibular incisors (Smith et al., 2019), we noticed expected sites of very uniform uniserial distributions of rows as well as instances of row peculiarities identical to those described by Risnes (1979b) and Moinichen et al. (1996). What was not expected and very surprising was the high frequency at which these row oddities were encountered especially in relation to short rows and to branching/merging of rows having the same tilt. The purpose of this investigation therefore was to characterize and quantify row distributions across the thickness of the inner enamel layer and as rows extend in a mesial and lateral direction toward the cementoenamel junctions (CEJ). The results based on single sections made from 24 different incisors will demonstrate that row distributions are considerably more irregular, variable and complex than heretofore realized. This study focuses on the 2D arrangement of the rows of rods with limited reflection into 3D in trying to interpret how the ameloblasts might form this arrangement.

Material and Methods

Ethical compliance

All procedures involving 7-week-old C57BL/6 wild type mice were reviewed and approved by the IACUC committee at the University of Michigan (UCUCA), and all aspects of the handling, care, and usage of 100 g male Sprague-Dawley wild type rats were carried out under guidelines specified by federal/provincial governmental agencies of Canada as approved by local animal care committees at McGill University.

Mouse Incisor Enamel Preparations

All data on the arrangement of rows of enamel rods in transverse sections of fully mineralized mandibular mouse incisor enamel were obtained from high resolution scanning electron microscope montage maps prepared for a previous investigation (Fig. 1 in Smith et al., 2019). Briefly, mice were fixed by vascular perfusion, the hemi-mandibles were removed and embedded in Epon 812 substitute plastic. One-mm-thick transverse sections from 18 right and 6 left mandibular incisors were prepared with a fine diamond saw at a site located 8 mm from the apical end of the incisor (Level 8, crest of alveolar bone near gingival margin). Care was taken to align the saw so that the slice was cut normal (perpendicular) to the enamel surface with minimal apical-to-incisal angulation and with minimal mesial-to-lateral angulation as was possible by free-hand dissection. Each section was re-embedded in castolite AC plastic and the incisal side of each block polished and etched. Overlapping images of the entire enamel layer from mesial to lateral CEJ were taken at x800 magnification in a Hitachi S-3000N variable pressure scanning electron microscope in backscatter mode. One montage map of the enamel layer from each of the 24 incisors were created in Adobe Photoshop (https://www.adobe.com) and rows of rods within the inner enamel layer were identified and color-coded by rod tilt (Fig. 1, mesial tilt= black, lateral tilt= red). The black and red color maps for each incisor were analyzed in ImageJ (https://imagej.nih.gov/ij/) using a standard threshold function and the polygon tracing function to outline the boundaries of each row of rods on the maps. Parameters quantified in scaled maps included the x- and y-coordinate centroid position of each enamel rod in the map, the number of rods per row (RPR) and the perpendicular distance in µm of the row from the DEJ measured from the lateral endpoint, the midpoint and the mesial endpoint of each row. Categorical variables used to classify 2D features of the rows in each map are described in Table 1. Data were collected and organized using MS Excel and then the completed files were opened in Statistica Version 13.3 for Windows (https://www.tibco.com/products/tibco-statistica) for routine analyses and graphing as well as for carrying out correspondence analyses of categorical variables (Sourial et al., 2010).

Rat Incisor Ameloblast Preparations

The curvature of the DEJ at the central labial aspect of mandibular mouse incisors is relatively high as it sweeps in mesial and lateral directions toward the CEJ at the extreme sides of the enamel layer (Fig. 1). In order to get less distorted, light-microscopic images of ameloblasts, Tomes processes and enamel cut in the tangential plane the incisor (cuts made parallel to the long axis of ameloblasts, see Nishikawa, 2017), we made use of unpublished data prepared from the mandibular incisors of rats from an old investigation (Smith and Warshawsky, 1977). Mandibular rat incisors were selected because they have a more extended and gentler curvature along the central labial side of the tooth compared to mandibular mouse incisors, but the enamel is almost the same thickness (Risnes, 1979b). Briefly, four male Sprague-Dawley weighing 100 g were perfused with 2.5% glutaraldehyde, the hemimandibles were removed, washed in neutral buffer, decalcified, osmicated and embedded in Epon. Sites on the mandibular incisors corresponding to where preameloblasts face little or no predentin (early presecretory stage of amelogenesis) and where differentiated ameloblasts start secreting the enamel layer (early secretory stage of amelogenesis) were sawed from the initial large area blocks, reoriented and glued onto fresh Epon stubs so that sections could be cut tangential to the enamel organ through the height of ameloblasts to the DEJ area. Serial 1-µm-thick sections were cut, transferred to glass slides and stained with toluidine blue. The first of the serial sections cutting though ameloblasts at the level of the distal junctional complex were identified and this section and subsequent sections in the series were photographed on 35 mm film. After development, the film strip was projected vertically onto graph paper and the outlines of ameloblasts as enhanced by the cut edges of the terminal web in interrow locations were traced onto the graph paper. The next section in the series was projected and the rectangular outlines of ameloblasts in this section were aligned to the previous section. Any new ameloblast appearing in the outer edges of the projection were drawn on the same graph paper. This procedure compressed the central labial curvature of the DEJ into a linear map and was continued thereby building up the mesial-to-lateral and apical-to-incisal dimensions until a much large map of the arrangement of ameloblasts in rows at the level of the distal junctional complex was obtained (as shown in Fig. 7D,E). The tangential maps were arbitrarily colored in magenta and green in Photoshop to illustrate the possible arrangement of rows into which different groups of ameloblasts might be organized.

Results

Basic Arrangement of Rows of Enamel Rods in Mandibular Mouse Incisors

The organization of enamel rods into rows having alternating tilt angles across the thickness of the inner enamel layer in transverse sections of rat and mouse incisors is well known and has been described in detail by many investigators including Boyde (1969), Warshawsky (1971), Risnes (1979b) and Moinichen et al. (1996) (Fig. 1A-C). The rows with alternating rod tilts are arranged vertically on top of each other and extend for varying distances in a mesial and/or lateral direction in the form of complete or partial semicircular arcs or mildly curvilinear and sometimes slightly wavy rows (Fig. 1B; Supporting Information Fig. S1). Arcing rows crossing the central labial aspect of the enamel layer rarely appeared symmetrical in the transverse plane and often showed a mesial arm arcing uniformly toward the DEJ and a more flattened lateral arm extending toward the outer enamel layer (Fig. 1B; Supporting Information Fig. S1). Several different types of row arrangements were evident in all regions of the enamel layer (Fig. 1; Table 1). These included occurrences where vertically adjacent rows rhythmically alternated between mesial and lateral tilts (Fig. 1C, U), where a row of either tilt appeared to branch into two rows or conversely, two rows having the same tilt merged into a single row (Fig. 1C, B), where two rows having the same tilt were paired with each other for variable distances and then were separated by other rows having the opposite tilt (Fig. 1C, P), and where rows of short length were situated above or below a companion row having the same rod tilt angle at one or more sites along the length of the companion row (Fig. 1C, F, the short row called a focal stack). Collectively, these row irregularities added variety, complexity and sense of row interlocking across the transverse plane to what, at a quick glance, seemed to be a reasonably symmetrical arrangement of rows.

Enamel Rods Not in Rows (Single Rods)

During initial analyses of row distributions, it became apparent that not all enamel rods could be assigned unequivocally to a specific row, that is, they appeared as isolated single rods within the inner enamel layer, often positioned at odd angles relative to neighboring rows (Fig. 2A, blue arrows; Table 2). On average there were 6 ± 4 orphaned enamel rods per incisor and they accounted for only 0.1% of the total enamel rod population analyzed (Table 2). Single rods had either a mesial tilt or a lateral tilt and were present at many sites across the transverse plane and thickness of the enamel layer (Fig. 2A-D). Single rods were most frequently found in the lateral region of the enamel layer, least frequent in the central region, and with variable frequency in the mesial region (Fig. 2C). In the lateral and central regions, the number of single rods having a mesial tilt was about equal to the number having a lateral tilt, whereas in the mesial region single rods having a lateral tilt were roughly 4 times more frequently encountered than single rods having a mesial tilt (Fig. 2C). Single rods having a lateral tilt also showed a

slightly positive trend to be present at sites located farther away from the DEJ in the mesial region of the inner enamel layer (Fig. 2D).

Distribution of Rows of Enamel Rods by Row Length (Number of Rods Per Row; RPR)

The total number of rows found within the inner enamel layer on each incisor in transverse sections varied widely (98-154 rows; Supporting Information Fig. S1). The grand mean for 24 incisors was 124 ± 15 rows per tooth equally distributed by tilt angle (Table 2). The number of rods per row was also highly variable on each incisor irrespective of rod tilt, from as little as 2 RPR to a maximum of 233 RPR (Fig. 3; Supporting Information Fig. S1). Three categories of row lengths were arbitrarily assigned for analytic purposes: short rows having 2-20 RPR, medium rows having 21-99 RPR, and long rows containing 100-233 RPR (Tables 1 and 3, Fig. 3). Roughly one-half of all rows identified (51%) were short in length, followed in frequency by medium rows (36%) and long rows (13%) (Table 3). As expected, short rows collectively accounted for only 10% of all enamel rods quantified, whereas medium and long rows accounted for about 45% each of the remaining 90% of all rods organized into rows (Table 3; Fig. 3). On a per incisor basis, the inner enamel layer on average was composed of long, medium and short rows in a ratio of 1:3:4 (Table 3). Computed by length class across all incisors, long rows contained on average 142 ± 32 RPR, medium rows 50 ± 22 RPR, and short rows 8 ± 5 RPR with no significant difference by rod tilt. Sequential alternating rows of rods were often of the same length class (short-short, medium-medium, long-long) but they never had the same value for row length (e.g., 5-5, 56-56, 150-150 were never observed).

Distribution of Rows of Enamel Rods by Region

In the initial phases of this investigation it quickly became evident that rows of enamel rods displayed three regional associations (Table 1), that is, 44% of all rows were present in the lateral region, 31% were associated with the central region and 25% were found in the mesial region (Table 3; Fig. 3). There was a slightly higher frequency of rows having a mesial tilt in the lateral region and rows having a lateral tilt in the mesial region caused primarily by differences in rod tilts for short rows (Table 3). The distribution of short, medium and long rows in each region was noticeably different (Table 3). The lateral and mesial regions were comprised mostly of short and medium rows whereas the central region was predominately related to medium and long rows (Table 3; Fig. 3). The ratios of short, medium and long rows in each region were distinctly different, that is, 1:6:12 long-medium-short in the lateral region,

1:1.6:2 short-long-medium in the central region and 1:2 medium-short for the mesial region. Because of the preponderance of short rows associated with the lateral and mesial regions and the lack of long rows in the mesial region, the majority of all enamel rods analyzed were found in rows associated with the central region (61% of all rods), followed by rows forming the lateral region (29% of all rods) and rows forming the mesial region (10% of all rods) (Table 3; Fig. 3).

Distribution of Rows by Row Type

Rows of enamel rods irrespective of tilt showed 5 distinct appearances and associations to neighboring rows (Tables 1 and 3; Fig. 4A). The row type most closely associated with a uniserial enamel pattern, termed a uniform row in this investigation, comprised only 22% of all rows and contained only 15% of all enamel rods analyzed (Table 3). The remaining 78% of rows containing 85% of all enamel rods in the inner enamel layer of mandibular mouse incisors were irregular and/or more complex in arrangement. The most frequent row type encountered was the focal stack, which accounted for 30% of all rows but because they were consistently petite rows (<40 RPR), they contained only 5% of all enamel rods analyzed (Table 3; Fig. 4A). They were usually nestled at the sides of longer rows having the same tilt (Fig. 1C and Fig. 4A). The other three more complex row types showed either pairing of two adjacent rows having the same rod tilt or branching/merging of one row into two rows, or vice versa, or a combination of both row pairing and branching/merging (Tables 1 and 3). Although not specifically analyzed in this investigation, most branching/merging rows showed only one such bifurcation along its length. The bifurcations in some cases bore a striking resemblance to the type of branching seen along human fingerprint ridges (Ramenzoni and Line, 2006). Rows associated with focal stacks were always preliminarily classified as paired. These three complex row types accounted for 49% of all rows and 81% of all enamel rods analyzed (Table 3). The least frequent row type found was simple branching/merging arrangement (7% of all rows containing 7% of all enamel rods analyzed; Table 3), whereas the second most frequent row type identified showed branching/merging plus pairing to another neighboring row having the same tilt (29% of all rows containing the majority, or 56%, of all enamel rods analyzed; Table 3; Fig. 4A).

The five row types were not uniformly distributed within the three regions of the enamel layer and there were distinct differences in row frequencies by row tilt (Fig. 4B). In broad terms, the row types most frequently found in the lateral region were focal stacks followed at half frequency by uniform rows, and rows that branched/merged and had sites of pairing to other rows of similar tilt (Fig. 4B). The most frequent row types identified in the central region were those that showed branching/merging and

pairing to other rows of similar tilt, followed at one-third frequency by rows paired to other rows with similar tilt and by uniform rows (Fig. 4B). The row types most frequently found in the mesial region were uniform followed closely by focal stacks and rows that showed branching/merging and pairing with other rows of similar tilt (Fig. 4B).

Distribution of Rows by Row Endpoint Locations

Rows of enamel rods irrespective of tilt showed 6 distinct arrangements of their mesial and lateral endpoints (Tables 1 and 3; Fig. 5A). The two most frequent endpoint relationships, which collectively accounted for 75% of all rows and 70% of all enamel rods analyzed, included one pattern where both endpoints were embedded somewhere within the inner enamel layer (IE-IE, most frequent; 55% of rows and 39% of all enamel rods) and another where one endpoint was close to the DEJ and the other endpoint was embedded somewhere inside the inner enamel layer (DEJ-IE, 20% of rows and 31% of all enamel rods; Table 3; Fig. 5A). The third most frequent arrangement was one where one endpoint was located somewhere within the inner enamel layer and the other endpoint extended to the boundary between the inner and outer enamel layers (IE-OE, 14% of rows and 18% of all enamel rods; Table 3; Fig. 5A). The remaining three arrangements (DEJ-DEJ, DEJ-OE, OE-OE) accounted for 11% of rows and 12% of all enamel rods analyzed (Table 3; Fig. 5A).

Similar to what was observed for row types, the six arrangements of row endpoints were not uniformly distributed within the 3 regions of the enamel layer and there were distinct differences in frequency by row tilt (Fig. 5B). The endpoints stretching from DEJ-DEJ were most abundant in the lateral region followed by the central region and in very low frequency in the mesial region (Fig. 5B). Rows having the DEJ-IE arrangement were found with highest frequency in the central region and around one-half the corresponding frequency in the lateral and mesial regions (Fig. 5B). Rows showing the DEJ-OE arrangement were rare and associated primarily with the central region (Fig. 5B). Rows having the IE-IE arrangement were found with highest frequency in the lateral region, and around one-half the corresponding frequency in the central and mesial regions (Fig. 5B). Rows with the IE-OE arrangement were found with highest frequency in the mesial region and with slightly lower frequency in the lateral and central regions (Fig. 5B). Lastly, rows showing the OE-OE arrangement were the second lowest in frequency and associated primarily with the lateral and mesial regions (Fig. 5B).

Correspondence Analyses by Row Tilt, Row Length, Regional Location, Row Type and Endpoint Location

Correspondence analyses of data for all row categorizations suggested several generalized intergroup relationships (Fig. 6). Row tilt occupies a central feature with mesial and lateral tilts equally distributed vertically above and below the origin on the 2D correspondence graphs (Fig. 6). Rows having a mesial tilt are most closely associated with the lateral region where the rows are medium or short in length, often in the form of a focal stack, and row endpoints are often buried within the inner enamel layer (IE-IE) or extending from DEJ-DEJ (Fig. 6). Rows having a mesial tilt are also associated, albeit less closely with the central region where the rows are generally organized in long or medium length rows that show branching/merging plus pairing with other rows having a mesial tilt. The endpoints of rows in the central region frequently extend from the DEJ into various locations within the inner enamel layer (DEJ-IE; Fig. 6). Rows having a lateral tilt are most closely associated with the mesial region where the rows are mostly medium in length and show simple branching or less often pairing with other rows having the same rod tilt or are uniform along their lengths (Fig. 6). The endpoints of shorter rows in the mesial region often extend from OE-OE and longer medium length rows travel from IE-OE or from DEJ-IE (Fig. 6).

Discussion

The Variable Nature Of 2D Transverse Row Arrangements In Mouse Mandibular Incisor Enamel

The results of this investigation were unexpected and very surprising considering the orderly arrangement of alternating row tilts implied to exist within the inner enamel layer of rat and mouse incisors, to the extent that deviations from a uniform uniserial pattern have been classified in the past as something abnormal (aberrations) (Risnes, 1979b). Figure 1 and Supporting Information Figure S1 illustrate that row arrangements, when considered on a more global context, the theme of organization within the inner enamel layer is irregularity and diversity in the length of rows and complexity in their spatial packing across the transverse plane of the incisor (Table 3). Very few rows of enamel rods stretch continuously from the mesial to lateral sides across the entire face of an incisor transverse section (2% of rows with RPR>180; Fig. 3 and Supporting Information Figure S1). Only 22% of all rows decussate with their neighboring rows in an orderly and uniform fashion (Table 3), and there were no instances in this investigation where uniformly decussating rows of enamel rods were arranged sequentially across the entire thickness of the inner enamel layer (Fig. 1, from DEJ toward OE; Supporting Information Fig. S1) (Risnes, 1979b). In addition, of the 24 incisors and 2,974 rows of enamel rods sampled (Table 2), we

found no cases where two neighboring rows with alternating (decussating) tilt angles possessed the exact same row length (same number of RPR in neighboring rows having alternating tilts). It has not been apparent from past literature that most rows of enamel rods in typical transverse sections of the inner enamel layer of mandibular mouse incisors are short in length (51% of all rows; Table 3) with many of the short rows arranged in the form of focal stacks nestled on the side of other longer rows having the same rod tilt (30% of all rows; Table 3; Fig. 1; Supporting Information Fig. S1).

The various row types described in this investigation are known (reviewed in Risnes, 1979b), but the high frequency of the more complex arrangements of row pairing, branching/merging, or both, and of the numerous focal stacks situated at the sides of longer rows having the same tilt angle are new insights into global row organization in mouse incisors. It is curious on a global basis that 35% of all rows are either uniform along their whole length or have sites of pairing to other rows having the same tilt angle (22% + 13%; Table 3), that 35% of all rows show some form of branching/merging (7% + 29%; Table 3), and that the remaining 30% of rows form petite focal stacks with other rows having the same tilt angle (Table 3). Notable also are the roughly comparable frequencies by tilt for all row types in the central region versus the high frequencies of rows having a mesial tilt for focal stacks in the lateral region and uniform rows in the mesial region (Fig. 4). This contrasts to the high frequencies of rows having a lateral tilt associated with paired rows in the lateral region and branching/merging plus paired rows as well as focal stacks in the mesial region (Fig. 4). The reasons for these higher frequencies are unknown.

The row types of special interest to this investigation are the branching/merging arrangement (with and without row pairing) and the focal stacks (Table 3; Fig. 4). The mode of development and functional significance of rows that branch/merge and have sites of row pairing is unknown (McIntyre et al., 2014, Varner and Nelson, 2014). These types of rows, if nothing else, add considerable variety and complexity to the packing of rows per unit volume within the inner enamel layer (Figs. 1 and 4; Supporting Information Fig. S1). Branching/merging of rows of enamel rods in Hunter-Schreger bands is an ancient pattern in mammalian enamel and, as noted in the Introduction, is especially prominent and complex in the enamel of ungulates. It has been associated most often with multiserial enamel where large groups of rods having same rod angulations spiral, twist or zigzag around one another (Rensberger and von Koenigswald, 1980, Sahni, 1985, von Koenigswald and Pfretzschner, 1987, Hanaizumi et al., 1996, Hanaizumi et al., 2010, Stefen and Rensberger, 1999, Jiang et al., 2003, Tabuce et al., 2007, von Koenigswald et al., 2011, Alloing-Séguier et al., 2014, Alloing-Séguier et al., 2017). Descriptions of branching/merging rows in uniserial enamel have been infrequent but one of the most dramatic

examples was presented by von Koenigswald and Pfretzschner (1987) in their Fig. 16 for European water vole incisor enamel from the late Pleistocene period (0.012-2.58 Ma). The enamel in these extant rodents resembles almost exactly the arrangements shown in Figure 1 and Supporting Information Figure S1. Row branching achieves at least two purposes. First, it increases the volume of space in which a row having one tilt angle can interact with rows having the opposite tilt angle; prior to the branch point two rows of opposing tilts lie above and below the branching row, whereas after the branch point there are five tilt transitions thereby increasing complexity. Second, a row having an opposite tilt is always wedged between the two arms of the branch point providing secure interlocking of the row nestled within the branchpoint (Fig. 1; Supporting Information Fig. S1). Branching is the most frequent feature of rows associated with the central region (Table 3; Fig. 4A and 6) and this may be one of the methods used to interlock rows developing in the lateral and mesial regions with rows projecting in both directions from the central region (Fig. 1; Supporting Information Fig. S1).

At first glance focal stacks seem to serve little purpose and may even represent sites of reduced fracture resistance within the inner enamel layer, but their high global frequency (Table 3) and richness in the lateral and mesial regions of the inner enamel layer suggest otherwise (Table 3; Fig. 4B). They may serve a simple purpose such as acting as a buffer to “fill-in” small spaces that development across the thickness of the inner enamel layer as it forms by appositional growth (movement of ameloblasts away from the DEJ). One aspect of focal stacks that needs clarification concerns whether the focal stacks extend the entire distance from near the DEJ to the enamel surface, as we suspect they do, or if they are truncated in length. There has been speculation that some enamel rods in rat and mouse incisor enamel may not extend the entire thickness of the enamel layer, but evidence for this has been weak (Alloing-Seguier et al., 2018). The origin of the focal stack arrangement may however be easier to explain. There is universal agreement by paleontologists that the uniserial enamel pattern in modern rat and mouse incisors evolved from a more ancient multilayered pattern, that is, multiple rows of enamel rods having the same tilt alternating with multiple rows of enamel rods having an opposite tilt. The debate has been whether the most primitive form was pauciserial or multiserial, arrangements distinguished by the direction of crystallites forming the interrod enamel (parallel versus angled to the rod crystallites, respectively) (Boyde, 1969, Sahni, 1985, von Koenigswald, 1985, Martin, 1993). The focal stacks could represent a remnant from the evolutionary change from the multi-row decussation pattern to the single-row decussation pattern reduced over millions of years to small clusters of enamel rods applied to sides of longer rows having the same tilt angle at various locations throughout the inner enamel layer.

Row Endpoints

It is not surprising that 55% of all rows seen in reasonably well oriented transverse sections have their two endpoints located somewhere between the DEJ and the OE (classified as IE-IE, Tables 1 and 3), that only 7% of all rows have their two endpoints both near the DEJ (DEJ-DEJ), and that only 3% of rows span the boundary with the outer enamel layer (OE-OE) since the former comprises the bulk of the inner enamel layer and the latter in a 3D context are narrow boundary areas between where rows start and where the row arrangement is lost in transition to outer enamel. What is surprising is that 34% of all rows show intermediate positioning of their endpoints, that is, spanning from near the DEJ to somewhere within the inner enamel layer (DEJ-IE, 20%) or from somewhere within the inner enamel layer to the boundary with the outer enamel layer (IE-OE, 14%). These two categories of row endpoint locations have remarkable similarities in their range and means for row lengths by rod tilt (data not shown), frequency, and distribution pattern of row lengths for each region of the inner enamel layer (Fig. 5B). Figure 5 further documents that sampling in 24 incisors was insufficient to obtain reliable statistical analyses in 3 out of the 6 categories defined for row endpoint locations; these are DEJ-DEJ and DEJ-OE in the mesial region, OE-OE in central region, and DEJ-OE in the lateral region where these rows were rarely encountered, probably in part because they comprised some of the longest rows observed in the central region and there are only a limited number of long rows in any give transverse section of the inner enamel layer (Table 3). The mesial region has no long rows, and these are present in only low frequency in the lateral region (Table 3; Fig. 3). Row lengths and endpoint distributions are also affected by plane of section, which is never perfectly aligned in the transverse plane (Smith et al., 2019). This is one the reasons for using 24 incisors in an attempt to obtain an overall representative sample. The exact pattern of row endpoint distributions will have to wait until the real 3D distribution pattern of rows can be defined by serial reconstructions of the whole enamel layer.

Row Interrelationships

The correspondence graphs in Figure 6 show several interesting interrelationships between row length, region, row type and row endpoint distributions. First, of the five categories of row endpoint ranges that could be analyzed all but two are in different quadrants of the graphs. The ones together are DEJ-IE and IE-OE, rows stretching into the inner enamel layer from the DEJ and out of the inner enamel layer to the boundary of the outer enamel layer. These share a relationship to medium length rows having lateral tilt and rows that often branch/merge or show pairing with other rows having the same tilt. Rows spanning DEJ-DEJ are variable in length, regional associations, and row tilt. Rows spanning the inner enamel layer (IE-IE) are most frequently short in length, often as a focal stack located in the lateral region and have a tendency for mesial tilt. Rows stretching across the boundary with the outer enamel

layer (OE-OE) are also frequently short in length, uniform, and located in the mesial region with a tendency for having a lateral tilt.

Implication of Row Lengths To Their Mode Of Formation

The 2D data in this investigation (Table 3) imply that as rows of ameloblasts form in the time intervals between the presecretory and secretory stages of amelogenesis, they become organized in a way to create various ratios of short, medium and long rows. On a global average basis this is 4 short, 3 medium and 1 long row per unit time of differentiation across the entire inner enamel layer starting near the DEJ. The process is considerably more complex than this because the three regions of enamel layer develop progressively over time with the central region starting first (equivalent to the cusp tip/incisal edge region of a human tooth) followed by the mesial region and the lateral region as the wave of differentiation spreads "sideways" toward the future sites of the CEJ and the labial side of the mouse incisor (Simmer et al., 2010). The mesial region is shorter in curvilinear length along the DEJ and therefore completes row formation before the wave of differentiation reaches the lateral CEJ (Smith and Warshawsky, 1976). As a result of these different timings in development, the ratio of short, medium and long rows in each region is much different compared to the global average. In the central region this ratio is 2 medium and 2 long rows for every short row, in the mesial region it is 3 short rows for every medium row, and in the lateral region it is 10 short rows and 6 medium rows for every long row (Table 3). It is tempting to speculate that the controlling factor in the row creation process is something that allows short groups of ameloblasts either to remain as they are or extend into medium length groups or into much longer groups by incorporating additional short ameloblast groups, but this aspect of possible developmental controls in the development of ameloblast rows remains to be more precisely defined as does the question of whether physical (Cox, 2013) or chemical (Kondo and Miura, 2010, Hiscock and Megason, 2015) factors control the development of row lengths and row tilts.

The Arrangement of Ameloblasts Into Rows

Considering the complexity and irregularity in row arrangement patterns within the inner enamel layer, an obvious question is whether similar irregularities extend to the organization of ameloblasts which produce the enamel rods. Many past investigators, especially Nishikawa in Japan, have argued that secretory stage ameloblasts are arranged in rows and the Tomes processes projecting from their distal ends show both row arrangement and differing row tilts (Boyde, 1969, Warshawsky, 1978, Hanaizumi et al., 1996, Hanaizumi et al., 2010, Risnes et al., 2002, Skobe, 2006, Yuan and Nishikawa, 2014, Nishikawa, 2017). Irregular row arrangements such as paired, branching/merging with or without row pairing, and focal stacks to the knowledge of the authors have not been described to any

extent in ameloblast row arrangements. Figure 7 illustrates that serial sections cut in the tangential plane of the incisor (sections cut parallel to the long axis of the ameloblasts) reveal short patches of the row arrangement in ameloblast when cut at the level of the distal terminal web (Fig. 7A) (Warshawsky, 1978, Yuan and Nishikawa, 2014, Nishikawa, 2017). Branching/merging of ameloblast rows is easily visible as are other rows extending across the field in more uniform fashion. There is also the suggestion of groups of ameloblasts lying at the sides of other ameloblast rows that may represent the equivalent of what will become a focal stack of enamel rods in production. Sections that cut at a level where Tomes processes are projecting into the forming enamel (Fig. 7B) show even more detail including mesial and lateral row tilts, row endpoints, rows that branch/merge or are in a paired arrangement with other rows having the same tilt (see also Warshawsky, 1978). These features all extend later in development into enamel rod row arrangements also clearly evident in tangential sections of maturing enamel (Fig. 7C). A more extensive view of ameloblast row arrangements prior to and during the early secretory stage is visible in 2D surface maps constructed from serial sections at the level of the distal terminal web (Fig. 7D,E; method of construction described in Materials and Methods). Early differentiating ameloblasts in the presecretory stage show a surprising high level of initial row organization that is noticeably wavy with individual ameloblasts in the rows appearing irregularly polygonal in outline at the level of the distal terminal web (Fig. 7D). The disorganized rows show the beginning of what is clearly branching/merging and sites where clusters of cells may represent the initial phases of delineating out new branching/merging sites reminiscent of patterns in development typical for the formation of mineralized structures in less complex organisms (McIntyre et al., 2014). Early secretory stage ameloblasts show a much more organized arrangement of rows, with the cells more regular and rectangular in outline (Fig. 7E) (Warshawsky, 1978, Yuan and Nishikawa, 2014). While row tilts cannot be defined at the level of the ameloblast terminal web, all row arrangements illustrated in Figure 4A for rows of enamel rods are evident in rows of ameloblasts at the very beginning of enamel secretion. The straightening out of the initial wavy rows of ameloblasts and of the ameloblasts themselves changing from irregular polygonal shape to a more rectangular shape at the distal terminal web provides two very simple physical methods, not requiring cell proliferation, to extend the rows outwards in the transverse plane (mesial-to-lateral direction) traditionally associated with gain in row length needed to prevent interrow spaces from developing internally as decussating rows move away from one another as the enamel rods are formed (discussed in Alloing-Séguier et al., 2018).

Development Of Rows Of Ameloblast Along The DEJ And Its Implication To Rod Decussation

The data from this investigation suggest that the reason why spaces do not develop because of physical sliding apart of two adjacent decussating rows of ameloblasts in rat and mouse incisors

(discussed in Boyde, 1969, Warshawsky, 1978, and Alloing-Séguier et al., 2018) is based on the manner in which row formation is induced and extended from the central region into the mesial and lateral regions at the level of the DEJ. This idea is schematically illustrated in Figure 8. The key element we suspect lies in the initial set up of the tilt angle of enamel rods forming for example in row A as it relates to the tilt angle of the next neighboring row B near the DEJ (Fig. 8). Once ameloblasts have defined these two angles they and all other ameloblasts in the same row move at this fixed tilt angle until the cells switch to forming the outer enamel portion of the enamel rod which has different transverse and sagittal tilt angles than the inner enamel portion (Fig. 8). At this changeover position, our hypothetical ameloblast A1 would now be positioned opposite a different ameloblast B2 that originated from an extension of the wave of differentiation spreading mesially earlier in time along the DEJ. The same happens for hypothetical ameloblast B1 which would be opposite to a different ameloblast A2 that originated from an extension of the wave of differentiation spread laterally along the DEJ also earlier in time (Fig. 8). The ameloblasts that are physically moving incisally (eruptive direction) and mesially or laterally away from one another maintain constant relationships to sister ameloblasts within the same row but they must constantly readjust their interrow relationships by mechanisms that remain poorly understood (Nishikawa, 2017). In this interpretation, space compensation for decussation-based separation distances is prebuilt into the system by creating and lengthening rows earlier in time along the DEJ as the wave of differentiation passes from central into the mesial and lateral regions, that is, as enamel formation first begins rather than after the ameloblasts in two adjacent decussating rows have moved in an incisal direction and physically apart from one another (Warshawsky, 1978). The fact that the decussation angles are different in the three regions of the enamel layer (Smith et al., 2019) makes 3D theoretical modeling of the path of enamel rods across the whole thickness of the enamel layer a very challenging mathematical problem (Fig. 8).

Summary and Conclusions

The results from this investigation have demonstrated that there is considerably more variety, complexity and irregularity in the arrangement of rows of enamel rods in mouse mandibular incisors than is acknowledged in the current view of the uniserial enamel pattern. These features include:

1. Rows of enamel rods are variable in length with 7 times as many rows half the length of the longest rows across the transverse plane of the incisor.
2. Most rows are curvilinear and slightly wavy and not linear across the transverse plane of the incisor.
3. Rows are not universally uniform along their whole length with perfectly alternating tilt angles; some rows having the same tilt become neighbors for variable distances (paired rows), some rows branch seamlessly into two rows, or two rows with the same tilt merge into each other, with a

row having the opposite tilt nested within the bifurcation point, some rows are both paired to other rows of similar tilt as well as branch/merge, and a large percentage of all rows (30%) are small in length and often found at the sides of other rows having the same tilt in the form of focal stacks.

4. Two neighboring rows with decussating tilt angles rarely have the same length (RPR).

5. Only 31% of rows in any transverse section lay within or cross the central region of the enamel layer where the wave of differentiation and subsequent process of amelogenesis first begin. Additional and generally shorter rows develop in the lateral region (44% of all rows) and in the mesial region (25% of all rows) as the wave of differentiation spreads transversely toward the lateral and mesial CEJ during development of the enamel layer.

6. Neighboring rows of enamel rods with decussating angles are formed by ameloblasts that move sideways in opposite directions. When the ameloblasts complete formation of the inner enamel layer, the rods they have formed are now located at a distance apart from one another dictated by the spread of the decussation angle specific for a given regional location across the thickness of the inner enamel layer. The rows of opposite tilt they now abut originated from other rows of enamel rods newly created near the DEJ as the wave of differentiation spread mesially and laterally away from site where first starting rows were located.

Acknowledgements

This study was supported by NIDCR/NIH grant 1R01DE015846 (J.CC.H.) and 1R01DE27675 (JPS). Raw coordinate data from this study can be obtained by emailing the primary author.

Conflict of interest

The authors declare no conflict of interest.

Author contributions

This study was designed principally by C.E.S. with contributions by J.P.S. and J.C-C.H. The incisors were prepared, sectioned, polished, and BEI-imaged by Y.H. Growth and mating of mice was overseen by J.C-

C.H. Data analysis and creating the first draft of the manuscript and figures was performed by C.E.S. The figures were modified by J.P.S. The manuscript was critically reviewed by J.C-C.H. and J.P.S.

References

Alloing-Séguier L, Lihoreau F, Boisserie J-R, Charruault A-L, Orliac M, Tabuce R (2014) Enamel microstructure evolution in anthracotheres (Mammalia, Cetartiodactyla) and new insights on hippopotamoid phylogeny. *Zool. J. Linn. Soc-Lond.,* **171,** 668–95.

Alloing-Seguier L, Marivaux L, Barczi JF, Lihoreau F, Martinand-Mari C (2018) Relationships Between Enamel Prism Decussation and Organization of the Ameloblast Layer in Rodent Incisors. *Anat Rec,* **26,** 24000.

Alloing-Séguier L, Martinand-Mari C, Barczi JF, Lihoreau F (2017) Linking 2D observations to 3D modeling of enamel microstructure–a new integrative framework applied to Hippopotamoidea evolutionary history. *J. Mamm. Evol.,* **24,** 221-31.

Boyde A (1969) Electron microscopic observations relating to the nature and development of prism decussation in mammalian dental enamel. *Bull Group Int Rech Sci Stomatol,* **12,** 151-207.

Cox BN (2013) How the tooth got its stripes: patterning via strain-cued motility. *J R Soc Interface.,* **10,** 20130266.

Goldberg M, Kellermann O, Dimitrova-Nakov S, Harichane Y, Baudry A (2014) Comparative studies between mice molars and incisors are required to draw an overview of enamel structural complexity. *Front. Physiol.,* **5,** Article 359.

Hanaizumi Y, Maeda T, Takano Y (1996) Three-dimensional arrangement of enamel prisms and their relation to the formation of Hunter-Schreger bands in dog tooth. *Cell Tissue Res.,* **286,** 103-14.

Hanaizumi Y, Yokota R, Domon T, Wakita M, Kozawa Y (2010) The initial process of enamel prism arrangement and its relation to the Hunter-Schreger bands in dog teeth. *Arch Histol Cytol,* **73,** 23-36.

Hiscock TW, Megason SG (2015) Orientation of Turing-like Patterns by Morphogen Gradients and Tissue Anisotropies. *Cell Syst.,* **1,** 408-416.

Jiang Y, Spears IR, Macho GA (2003) An investigation into fractured surfaces of enamel of modern human teeth: a combined SEM and computer visualisation study. *Arch Oral Biol.,* **48,** 449-57.

Kawai N (1955) Comparative anatomy of the bands of Schreger. *Okajimas Folia Anat Jpn.,* **27,** 115-31.

Kondo S, Miura T (2010) Reaction-diffusion model as a framework for understanding biological pattern formation. *Science.,* **329,** 1616-20.

Lynch CD, O'Sullivan VR, Dockery P, McGillycuddy CT, Sloan AJ (2010) Hunter-Schreger Band patterns in human tooth enamel. *J Anat.,* **217,** 106-15.

Lyngstadaas SP, Moinichen CB, Risnes S (1998) Crown morphology, enamel distribution, and enamel structure in mouse molars. *Anatomical Record,* **250,** 268-80.

Martin T (1993) Early rodent incisor enamel evolution: Phylogenetic implications. *J Mam Evol,* **1,** 227-254.

Martin T (1999) Evolution of incisor enamel microstructure in Theridomyidae (Rodentia). *J Ver Paleo,* **19,** 550-565.

Martin T (2007) Incisor Enamel Microstructure and the Concept of Sciuravida. *Bull. Carnegie Mus. Nat. Hist.,* **2007,** 127-141.

McIntyre DC, Lyons DC, Martik M, McClay DR (2014) Branching out: origins of the sea urchin larval skeleton in development and evolution. *Genesis.,* **52,** 173-85.

Moinichen CB, Lyngstadaas SP, Risnes S (1996) Morphological characteristics of mouse incisor enamel. *J. Anat.,* **189,** 325-33.

Nishikawa S (2017) Cytoskeleton, intercellular junctions, planar cell polarity, and cell movement in amelogenesis. *J Oral Biosci,* **59,** 197-204.

Osborn JW (1970) The mechanism of ameloblast movement: a hypothesis. *Calcif Tissue Res,* **5,** 344-59.

Osborn JW (1990) A 3-dimensional model to describe the relation between prism directions, parazones and diazones, and the Hunter-Schreger bands in human tooth enamel. *Arch Oral Biol,* **35,** 869-78.

Radlanski RJ, Renz H (2006) Developmental movements of the inner enamel epithelium as derived from micromorphological features. *Eur J Oral Sci,* **114 Suppl 1,** 343-8.

Ramenzoni LL, Line SR (2006) Automated biometrics-based personal identification of the Hunter-Schreger bands of dental enamel. *Proc Biol Sci.,* **273,** 1155-8.

Rensberger JM, von Koenigswald W (1980) Functional and phylogenetic interpretation of enamel microstructure in rhinoceros. *Paleobiology,* **6,** 477-495.

Risnes S (1979a) A method of calculating the speed of movement of ameloblasts during rat incisor amelogenesis. *Arch Oral Biol,* **24,** 299-306.

Risnes S (1979b) A scanning electron microscope study of aberrations in the prism pattern of rat incisor inner enamel. *Am J Anat,* **154,** 419-36.

Risnes S, Septier D, Deville de Periere D, Goldberg M (2002) TEM observations on the ameloblast/enamel interface in the rat incisor. *Connect Tissue Res,* **43,** 496-504.

Sahni A (1985) Evolutionary trends in the enamel of rodent incisors. In *Evolutionary Relationships among Rodents: A Multidisciplinary Analysis* (eds Luckett WP, Hartenberger J-L), pp. 133-150. NY: Springer Science.

Simmer JP, Papagerakis P, Smith CE, et al. (2010) Regulation of dental enamel shape and hardness. *J. Dent. Res.,* **89,** 1024-38.

Skobe Z (2006) SEM evidence that one ameloblast secretes one keyhole-shaped enamel rod in monkey teeth. *Eur J Oral Sci,* **114 Suppl 1,** 338-42.

Smith CE, Hu Y, Hu JC, Simmer JP (2019) Quantitative analysis of the core 2D arrangement and distribution of enamel rods in cross-sections of mandibular mouse incisors. *J Anat.,* **234,** 274-290.

Smith CE, Warshawsky H (1976) Movement of entire cell populations during renewal of the rat incisor as shown by radioioautography after labeling with 3H-thymidine. The concept of a continuously differentiating cross-sectional segment. (With an appendix on the development of the periodontal ligament). *Am. J. Anat.,* **145,** 225-59.

Smith CE, Warshawsky H (1977) Quantitative analysis of cell turnover in the enamel organ of the rat incisor. Evidence for ameloblast death immediately after enamel matrix secretion. *Anat. Rec.,* **187,** 63-98.

Sourial N, Wolfson C, Zhu B, et al. (2010) Correspondence analysis is a useful tool to uncover the relationships among categorical variables. *J Clin Epidemiol.,* **63,** 638-46.

Stefen C, Rensberger JM (1999) The specialized enamel structure of hyaenids (Mammalia, Hyaenidae): Description and development within the lineage - Including percrocutids. *Scanning Micros.,* **13,** 363-380.

Tabuce R, Delmer C, Gheerbrant E (2007) Evolution of the tooth enamel microstructure in the earliest proboscideans (Mammalia). *Zool. J. Linn. Soc-Lond.,* **149,** 611-628.

Tomes J (1850) On the structure of the dental tissues of the order rodentia. *Phil. Trans. R. Soc. Lond.,* **140,** 529-567.

Varner VD, Nelson CM (2014) Cellular and physical mechanisms of branching morphogenesis. *Development.,* **141,** 2750-9.

Vieytes EC, Morgan CC, Verzi DH (2007) Adaptive diversity of incisor enamel microstructure in South American burrowing rodents (family Ctenomyidae, Caviomorpha). *J Anat.,* **211,** 296-302.

von Koenigswald W (1985) Evolutionary trends in the enamel of rodent incisors. In *Evolutionary Relationships among Rodents: A Multidisciplinary Analysis* (eds Luckett WP, Hartenberger J-L), pp. 403-422. New York: Springer Science.

von Koenigswald W, Clemens WA (1992) Levels of complexity in the microstructure of mammalian enamel and their application in studies of systematics. [Review]. *Scanning Microsc.,* **6,** 195-217.

von Koenigswald W, Holbrook LT, Rose KD (2011) Diversity and evolution of Hunter – Schreger Band configuration in tooth enamel of perissodactyl mammals. *Acta Palaeontol. Pol.,* **56,** 11-32.

von Koenigswald W, Pfretzschner HU (1987) Hunter-Schreger-Bänder im Zahnschmelz von Säugetieren (Mammalia). *Zoomorphology,* **106,** 329-38.

von Koenigswald W, Rensberger JM, Pretzschner HU (1987) Changes in the tooth enamel of early Paleocene mammals allowing increased diet diversity. *Nature,* **328,** 150-2.

Warshawsky H (1971) A light and electron microscopic study of the nearly mature enamel of rat incisors. *Anat. Rec.,* **169,** 559-83.

Warshawsky H (1978) A freeze-fracture study of the topographic relationship between inner enamel-secretory ameloblasts in the rat incisor. *Am J Anat.,* **152,** 153-207.

Yahyazadehfar M, Bajaj D, Arola DD (2013) Hidden contributions of the enamel rods on the fracture resistance of human teeth. *Acta Biomater.,* **9,** 4806-14.

Yilmaz ED, Schneider GA, Swain MV (2015) Influence of structural hierarchy on the fracture behaviour of tooth enamel. *Philos Trans A Math Phys Eng Sci.,* **373,** rsta.2014.0130.

Yuan X, Nishikawa S (2014) Angular distribution of cross-sectioned cell boundaries at the distal terminal web in differentiating preameloblasts, inner enamel secretory ameloblasts and outer enamel secretory ameloblasts. *Microscopy (Oxf).* **63,** 33-9.

Supporting Information Figure S1. Color maps showing similarities and differences in the arrangement of rows of enamel rods having a mesial tilt (black) and lateral tilt (red) on 4 out of the 24 incisors analyzed in this investigation (Incisors T2, T7, T15, T20).

TABLE 1: CATEGORICAL VARIABLES USED FOR CLASSIFYING ROWS OF ENAMEL RODS IN THE INNER ENAMEL LAYER OF MANDIBULAR MOUSE INCISORS

A. INCISOR NUMBER (tooth 1-24)

B. ROW TILT (1= mesial, 2= lateral)

C. ROW NUMBER (row 1-154, the maximum row count detected for a given tooth in the 24 incisors analyzed)

D. ROW LENGTH expressed as rods per row (RPR)

1= SHORT (2-20 RPR)

2= MEDIUM (21-99 RPR)

3= LONG (100-233)

E. REGION where row is located based on normalized X-axis location of row (Fig. 1, Vx):

1= LATERAL, Vx of mesial row endpoint <0.6

2= CENTRAL, Vx of mesial row endpoint >0.5999 or lateral row endpoint <0.6999

3= MESIAL, Vx of lateral row endpoint >0.6999

F. ROW TYPE

1= rows is UNIFORM across its whole length with opposite tilt angles in rows above and below

2= two rows with the same row tilt are PAIRED with each other for short distances at one or more locations across their transverse lengths

3= row appears to branch (bifurcate) into two rows having the same rod tilt or two rows with same tilt appear to merge into one row having same rod tilt depending upon the transverse direction in which the row is viewed (BRANCH/MERGE)

4= rows appear to branch/merge with two other rows have same rod tilt as well as have sites where they are paired with other rows having the same row tilt (BRANCH/MERGE + PAIRED)

5= a row with petite length appears positioned above or below another row having same rod tilt (called a FOCAL STACK)

G. ROW RANGE

1= DEJ-DEJ, mesial and lateral row endpoints almost touch the DEJ

2= DEJ-IE, one row endpoint almost touches the DEJ and the other row endpoint is buried within inner enamel layer

3= DEJ-OE, one row endpoint almost touches the DEJ and the other row endpoint extends to the boundary with the outer enamel layer

4= IE-IE, both row endpoints are within the inner enamel layer

5= IE-OE, one row endpoint is within the inner enamel layer and the other row endpoint is at the boundary with the outer enamel layer

6= OE-OE, both row endpoints are at the boundary with the outer enamel layer

TABLE 2: OVERALL 2D GLOBAL ORGANIZATION OF ENAMEL RODS IN THE INNER ENAMEL LAYER OF MANDIBULAR MOUSE INCISORS

	Average Per Incisor[A]	Sum of All Incisors[A]
Number of rods per cross section	5,102 ± 397	122,438 (100%)
As isolated single rods	6 ± 400	143 (0.1%)
In rows with 2-233 rods per row (RPR)[B]	5,096 ± 395	122,295 (99.9%)
Mesial tilt	2,687 ± 232	64,480 (53%)
Lateral tilt	2,409 ± 204	57,815 (47%)
Number of rows per cross section[B]	124 ± 15	2,974 (total rows)[A]
Mesial tilt	62 ± 7	

	Lateral tilt	62 ± 9				

[A]N=24

[B]Data from Smith et al., 2019

TABLE 3: 2D DISTRIBUTION OF ROWS OF ENAMEL RODS IN THE INNER ENAMEL LAYER OF MANDIBULAR MOUSE INCISORS BY ROW ATTRIBUTES

	Average Per Incisor			Sum of All Incisors[A]	
ROW ATTRIBUTES:	Total	Mesial Tilt	Lateral Tilt	Total Rows	Total Rods
	Number of rows per cross section ± SD[B]				
ROW LENGTH					
Short (2-20 RPR[C])	63 ± 11	31 ± 6	32 ± 7	1,514 (51%)	12,788 (10%)
Med (21-99 RPR)	45 ± 70	22 ± 4	22 ± 4	1,069 (36%)	53,870 (44%)
Long (100-233 RPR)	16 ± 20	9 ± 2	7 ± 2	391 (13%)	55,637 (46%)
ROW REGIONAL LOCATION					
Lateral	54 ± 8	30 ± 5	25 ± 5	1,302 (44%)	35,449 (29%)
Short	33 ± 6	19 ± 3	14 ± 5	801 (27%)[62%][D]	
Medium	18 ± 4	9 ± 3	9 ± 2	435 (15%) [33%]	
Long	3 ± 2	1 ± 1	2 ± 1	66 (2%) [5%]	
Central	39 ± 4	20 ± 2	19 ± 3	931 (31%)	74,282 (61%)
Short	8 ± 3	4 ± 2	4 ± 2	192 (6%) [21%]	
Medium	17 ± 3	8 ± 2	9 ± 2	414 (14%) [44%]	
Long	14 ± 2	8 ± 1	6 ± 2	325 (11%) [35%]	
Mesial	31 ± 7	13 ± 4	18 ± 4	741 (25%)	12,564 (10%)
Short	22 ± 6	7 ± 3	14 ± 4	521 (18%) [70%]	
Medium	9 ± 3	5 ± 2	4 ± 2	220 (7%) [30%]	
ROW TYPE					

	Uniform	27 ± 6	14 ± 4	14 ± 3	651 (22%)	17,949 (15%)
	Paired	16 ± 5	6 ± 2	10 ± 4	384 (13%)	21,636 (18%)
	Branch/merge	9 ± 4	5 ± 3	4 ± 2	209 (7%)	8,887 (7%)
	Branch/merge+paired	36 ± 6	18 ± 4	17 ± 5	852 (29%)	67,940 (56%)
	Focal stack	37 ± 7	19 ± 4	18 ± 5	878 (30%)	5,883 (5%)
ROW ENDPOINT LOCATIONS						
	DEJ to DEJ	9 ± 3	4 ± 2	4 ± 1	212 (7%)	7,799 (6%)
	DEJ to IE	25 ± 4	13 ± 2	12 ± 3	591 (20%)	37,355 (31%)
	DEJ to OE	1 ± 2	1 ± 1	1 ± 1	30 (1%)	4,842 (4%)
	IE to IE	68 ± 10	35 ± 6	34 ± 6	1,639 (55%)	47,561 (39%)
	IE to OE	17 ± 7	8 ± 4	9 ± 4	415 (14%)	22,215 (18%)
	OE to OE	4 ± 2	2 ± 1	2 ± 1	87 (3%)	2,523 (2%)

[A]N=24

[B]SD= standard deviation

[C]RPR= rods per row

[D][Percentage composition of region]

Legends to Figures

Figure 1. Backscattered scanning electron microscopic (BEI) images of a right mandibular mouse incisor in transverse section viewed looking in an apical direction (toward growing apical end) and photographed at low and high magnification (A,B), and a cropped portion of the inner enamel layer from the central labial side of the incisor (C). Panel A, single low magnification BEI image of labial side of a mandibular mouse incisor in a typical transverse section of the tooth showing the location of dentin and enamel. The cracks in the dentin are an artifact caused by air drying the tissue slice after polishing. Panel B, a high-resolution map of the same tooth section shown in Panel A made from BEI images photographed at x800 and montaged to recreate the whole enamel layer. The cut open oval profiles of enamel rods are arranged in rows across the inner enamel layer between the limits of the mesial and lateral cementoenamel junctions (CEJ). The enamel rods are colored black for rows having a mesial tilt and red for rows having a lateral tilt. The mesial endpoints (MEP) and lateral endpoints (LEP) of the rows are color coded green for

rows having a mesial tilt and yellow for rows having a lateral tilt. Superimposed over the image are the x- and y-axes of a graph illustrating the normalized virtual coordinate system (Vx, Vy) used for defining the locations of individual rods or regions of the inner enamel layer: lateral region to the left of the vertical yellow line, central region within the two vertical yellow lines and mesial region to the right of second vertical yellow line (see Table 1 for classification details). Panel C, the rows of enamel rods show a variety of arrangements including uniform appearance along their length with opposite tilt angles in rows above and below (U), sites where two rows with the same tilt come into close proximity to each other (paired) (P), rows that appear to branch into two rows with the same tilt or where two rows with same tilt merge into one row (B), and sites where petite rows appear located at the sides of longer rows having the same tilt (called focal stacks, F). Key: DEJ, dentinoenamel junction; OE, outer enamel.

Figure 2. Distribution of single enamel rods that could not be assigned to a specific row. In every transverse section examined in this investigation, there were always some instances where single enamel rods appeared out of alignment to neighboring rows. Panel A, cropped area in the lateral region of the inner enamel layer showing rows of enamel rods having either mesial (black) or lateral (red) tilts. Many of the rows show uniform alternation of row tilts (e.g., 1-2-3-4) but there are cases where two rows with same tilt are paired with other (e.g., rows 4-5) and other irregularities where a row terminates (green, row endpoint for row with mesial tilt; yellow, row endpoint for row with lateral tilt) as well as cases where single enamel rods appear out of alignment with other neighboring enamel rods having similar tilt (black S1 with blue arrow for mesial tilt; red S2 with blue arrow for lateral tilt). Yellow arrows, sheets of interrod enamel; OE= outer enamel layer. Panel B, scatter plot in virtual coordinates illustrating sites where out-of-alignment single enamel rods were found in the 24 incisors examined. Panel C, bar graph showing the frequency of single enamel rods relative to rod tilt (blue=mesial, orange=lateral) and the three regions of the enamel layer. Numbers below regions indicate ratio of mesial tilt to lateral tilt, numbers on top of graph indicate total enamel rods irrespective of tilt. Panel D, scatter plot with linear correlation lines for single rods relative to their x-axis location and distance away from the DEJ (y-axis) as measured in scaled montage maps.

Figure 3. Graphic representations of Figure 1B illustrating the distribution of short, medium, and long rows and the distributions of rows in the lateral, central and mesial regions of the inner enamel layer. Criteria for classifying rows by length and region are shown in Table 1. The percentages in

each category for all 24 incisors analyzed are indicated. The arrows point to the longest row having a mesial tilt (black) and a lateral tilt (red) found on this tooth.

Figure 4. Graphic representations of Figure 1B showing the distribution of the five row types classified by the region of the inner enamel layer in which they are located (Panel A). An enlarged cropped area of the central region is shown at the top of the panel. Criteria for classifying rows by region and by row type are shown in Table 1. Panel B, bar graphs showing the frequency distribution in all 24 incisors analyzed for row types associated with the lateral, central and mesial regions. Row types: Uni, uniform; Par, paired; Bm, branch/merge; P+B, paired+branch/merge; FS, focal stack. Mtilt, rows with mesial tilt; Ltilt, rows with lateral tilt.

Figure 5. Graphic representations of Figure 1B showing the distribution of the six arrangements of row endpoints classified by the region of the inner enamel layer in which they are located (Panel A). An enlarged cropped area of the central region is shown at the top of the panel. Criteria for classifying rows by region and row range are shown in Table 1. Panel B, bar graphs showing the frequency distribution in all 24 incisors analyzed for row endpoint locations associated with the lateral, central and mesial regions. DEJ, dentinoenamel junction, IE, inner enamel layer, OE, outer enamel layer.

Figure 6. Correspondence plots of 2D relationships between categorical variables for row tilt, row class (length), enamel layer region, row type (A) or row endpoint location (range, B). Row tilt, row class (length) and enamel layer region have similar interrelationships in the two plots. Row type and row range also show similar single factor distribution with one category in every quadrant and second category in the southwest quadrant: paired and branching/merging rows in the case of A and DEJ-IE and DEJ-OE in the case of B. B/M, branch/merge; Stk, stack.

Figure 7. One µm thick tangential sections (plastic) of secretory stage rat incisor ameloblasts at the level of their distal terminal webs (A) and at the level of the Tomes processes projecting into the forming enamel layer (B), and in nearly mature enamel from the maturation stage (C) stained with toluidine blue. The tilt of a row cannot be defined in Panel A but uniform rows (u), branching/merging rows (b), and sites where a focal stack might be located (f) are apparent. Tomes processes projecting into the forming enamel layer from secretory stage ameloblasts (B) show many of the row arrangements typically identified later in enamel rod arrangements (C) that develop from these distal extensions of the ameloblasts. This includes uniform rows (u), branching/merging rows (b), paired rows (p) and focal stacks (f). In B and C, the endpoint for rows having a mesial tilt are indicated in green with black outline and for rows having a lateral

tilt in yellow with red outline. The colored maps in Panels D and E are graphic reconstructions from serial sections (see Materials and Methods) of the row arrangement of ameloblasts at the level of the distal terminal web in young differentiating ameloblasts (D) and in early secretory stage ameloblasts (E). The development of rows of ameloblasts clearly begins very early as preameloblasts start to differentiate (Panel D) with focal areas where cells seem clustered (c) at sites that may have something to do with branching/merging of rows seen more clearly later in time (Panel D). As secretion of the enamel begins (E), row structure is more regular and spread out as uniform (u), paired (p), branching/merging (b) and focal stack (f) patterns. In all panels the magnification bars = 25 µm, apical is to the left, incisal to the right, lateral to the top, and mesial to the bottom.

Figure 8. Schematic illustrations of enamel rod decussation taking into account increases in the mean decussation angle from lateral to mesial regions of the inner enamel layer (46°, 54°, 74°; Smith et al., 2019) for the whole enamel layer (A) and central region only (B). Rows of ameloblasts that form the rows of enamel rods undergo their differentiation as the wave of tooth development spreads from central region toward the mesial and lateral regions of the future enamel layer (e.g., red and black arrows labeled +53 µm in top figure). Rows therefore are created and lengthen at sites close to the DEJ. A transverse section of the mature enamel layer is a time composite image of all the various generations of ameloblasts that were required to create the rows of rods layered one-on-top another. This implies that two neighboring ameloblasts, one from a row destined to form an enamel rod having a mesial tilt (black, A1) and the other from a row creating enamel rods having a lateral tilt (red, B1) spread apart by a distance that can be estimated from planar geometry using decussation angle and the thickness of the enamel layer over which the cells will travel (blue triangles). As these ameloblasts and their sister cells in the same row move to form a corresponding row of enamel rods, new ameloblasts continue to develop near the DEJ along the same row or as part of new rows having similar rod tilts (A2 and B2). At the boundary area where ameloblasts switch from forming the decussating inner enamel portions of the rods to forming the parallel outer enamel portions of the rods, ameloblast A1 will oppose ameloblast B2 that differentiated at a more mesial spatial location than ameloblast B1, and ameloblast B1 will oppose ameloblast A2 that differentiated at a more lateral location than ameloblast A1. This implies that the potential space that would arise as ameloblasts in row A physically move in a mesial direction over space and time from ameloblasts in row B moving laterally is pre-compensated for by transverse extensions of arcing rows and creation of new rows as the wave of amelogenesis spreads into the mesial and lateral regions along the DEJ. It is

important to keep in mind that because enamel rods are tilted incisally (forwards) at about 45° to the DEJ in the plane of tooth eruption, the START positions for rows of rods at the DEJ in 3D space are positioned at least 100 µm more apically (backwards into the plane of the photographs shown here) than their END locations at the boundary with the outer enamel layer. It is not possible to see the start and end positions of an enamel rod in a single 2D section as represented in this figure, which is strictly for conceptual purposes.

Supporting Information Figure S1. Color maps showing arrangement of rows of enamel rods having a mesial tilt (black) and lateral tilt (red) in 4 out of the 24 incisors analyzed in this investigation (Incisors T2, T7, T15, T20). The distribution of rows of enamel rods across the transverse plane is noticeably variable. Rows with mesial tilt almost never have the exact same total number of enamel rods, the same total number of rows, or the same lengths (expressed as rods per row; RPR) forming the longest rows compared to rows having a lateral tilt both within and between incisors. There are, however, common themes in row organization including the non-linear and often wavy appearance of most rows, the arcing of rows across the central region (C) with variable arms extending into the mesial (M) and lateral (L) regions, the existence of some rows traversing only the mesial region (T7, black arrow for mesial tilt, red arrow for lateral tilt) or the lateral region (T15, black arrow for mesial tilt, red arrow for lateral tilt). The mesial region also shows distinct layering of rows towards the outer part of the inner enamel layer (T7, black and red arrows). Color code for small arrows: green, mesial and lateral endpoints for longest rows; magenta, uniform rows; dark blue, paired rows; muddy orange, branching/merging rows; cyan, branching/merging plus paired rows; dark red, focal stacks (classifications explained in Table 1).

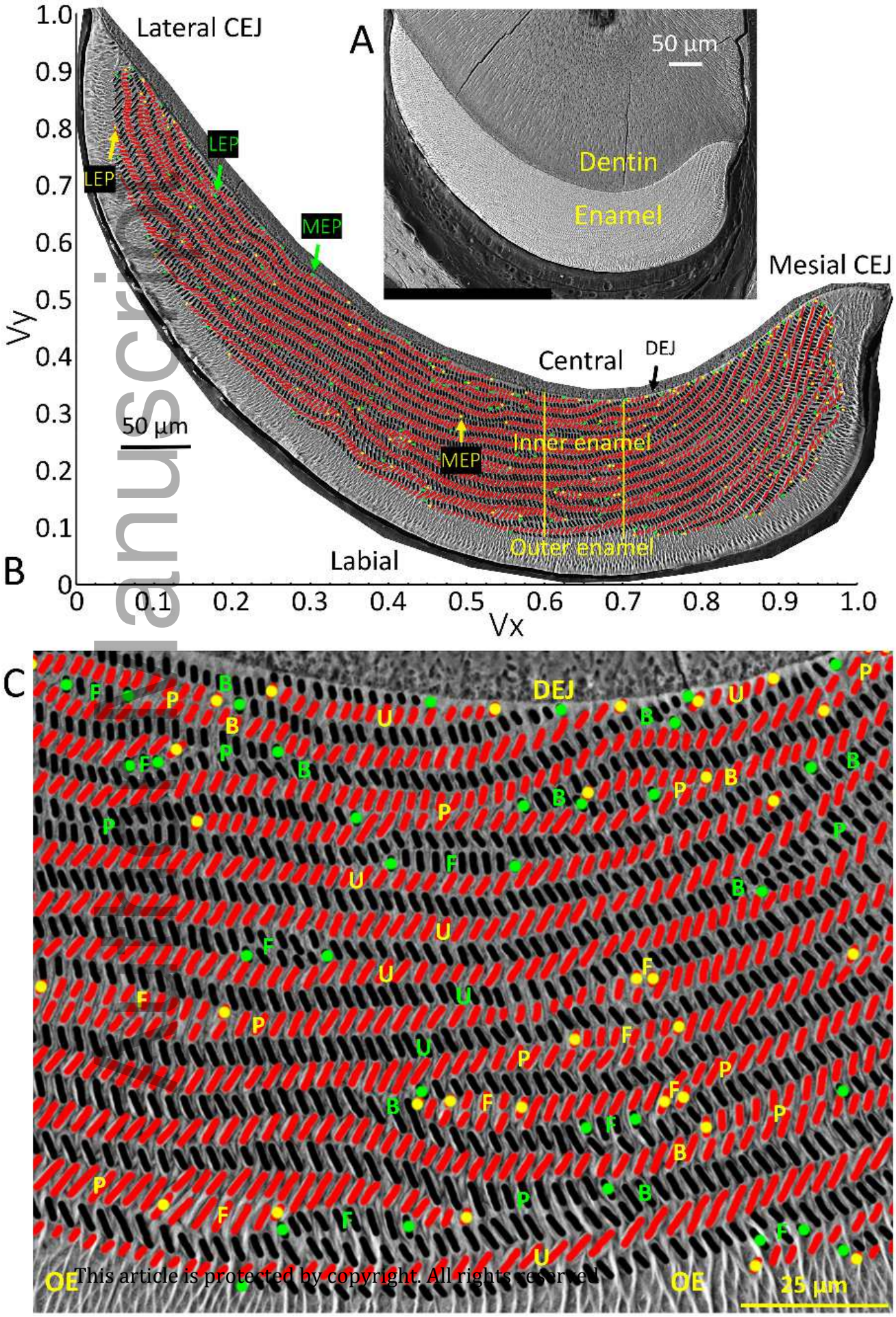

joa_13053_f1.tif

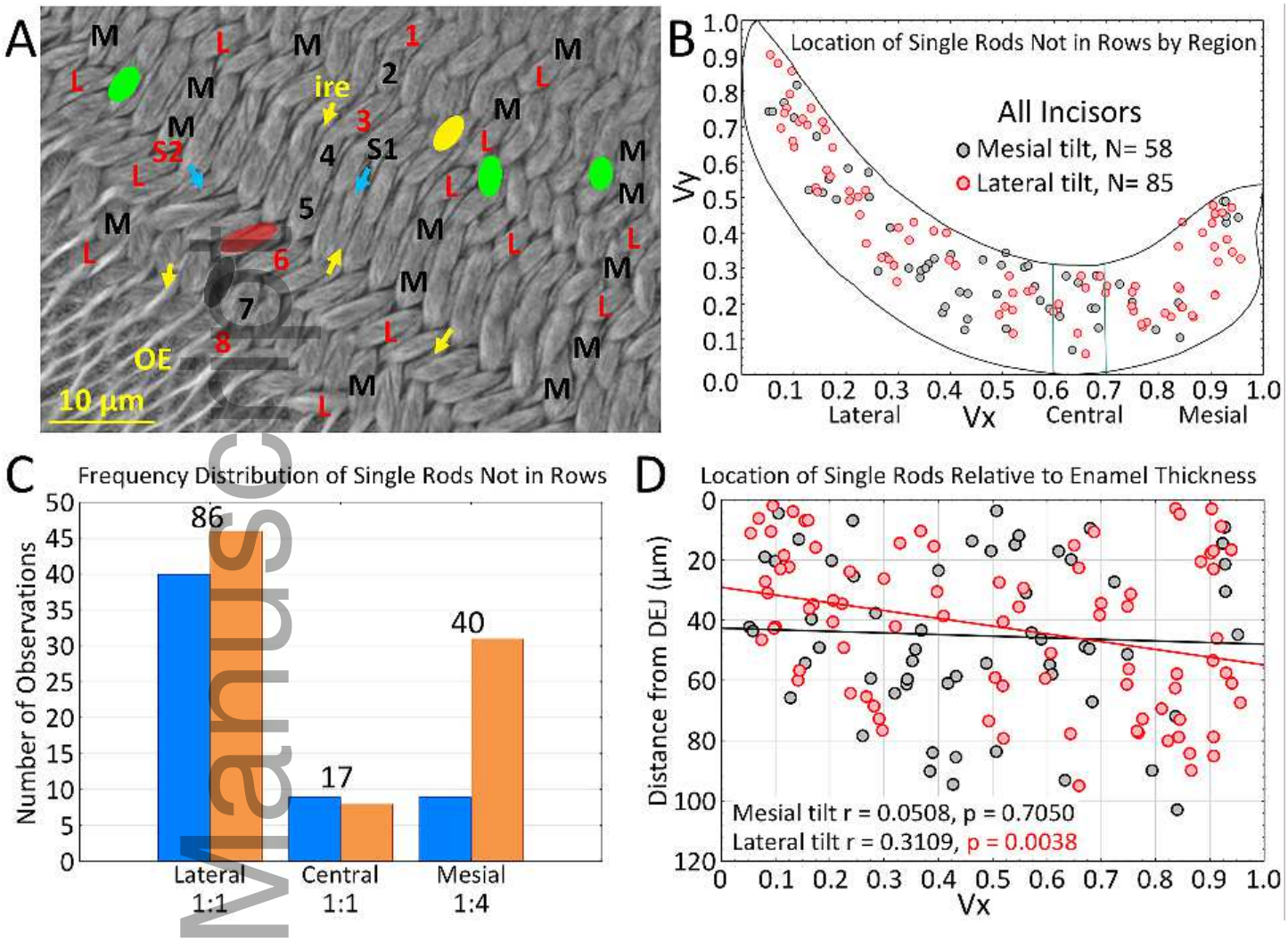

joa_13053_f2.tif

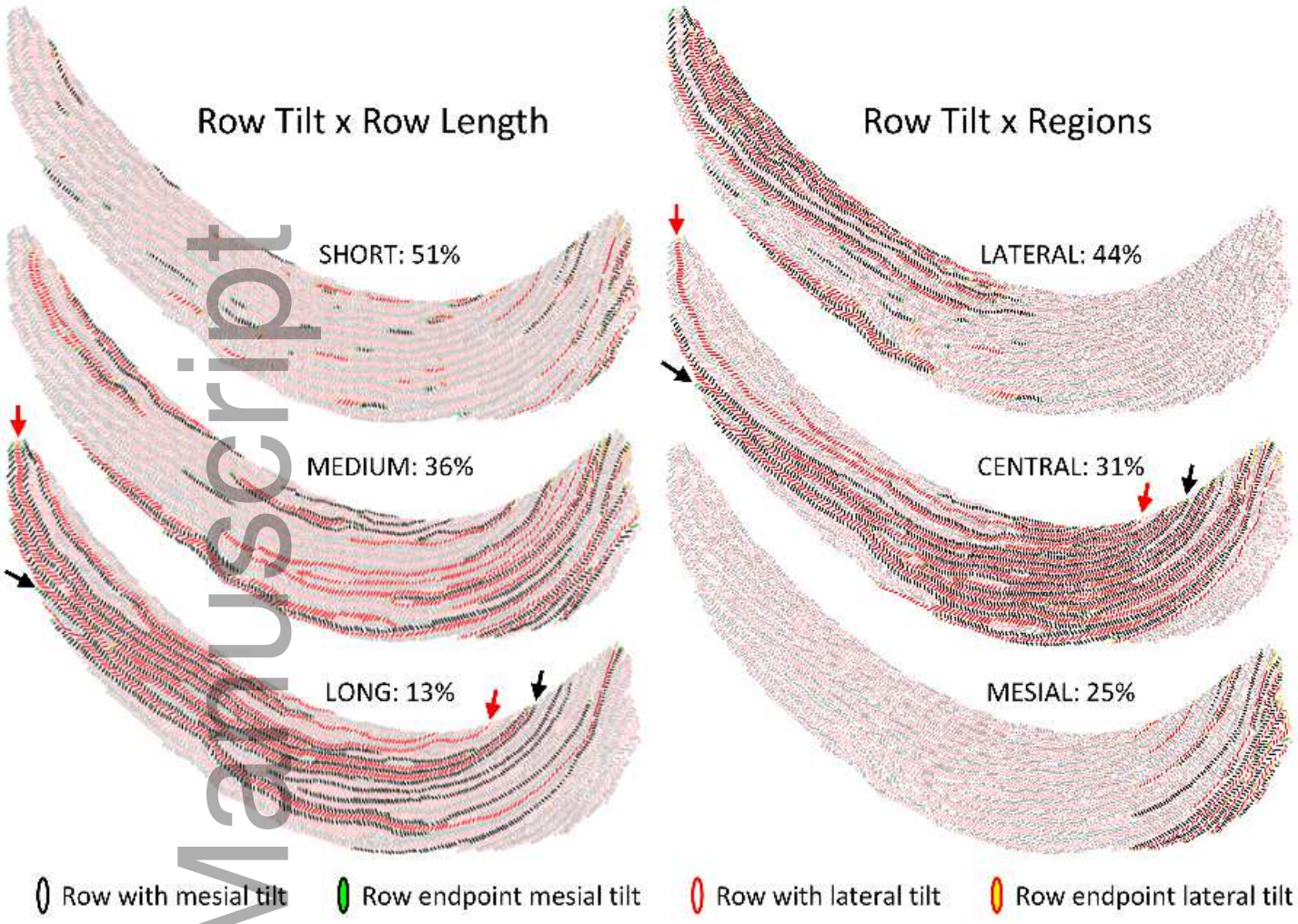

joa_13053_f3.tif

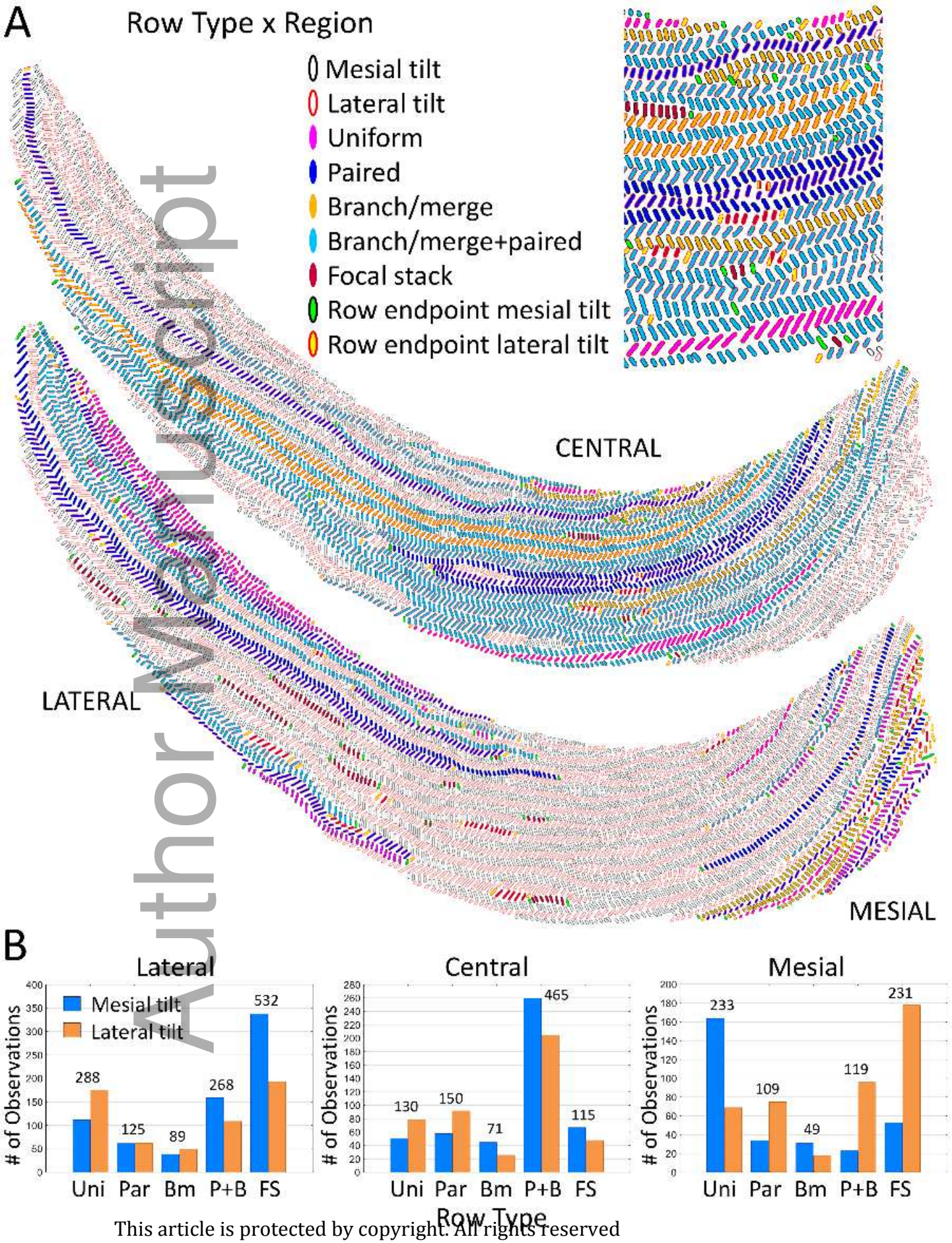

joa_13053_f4.tif

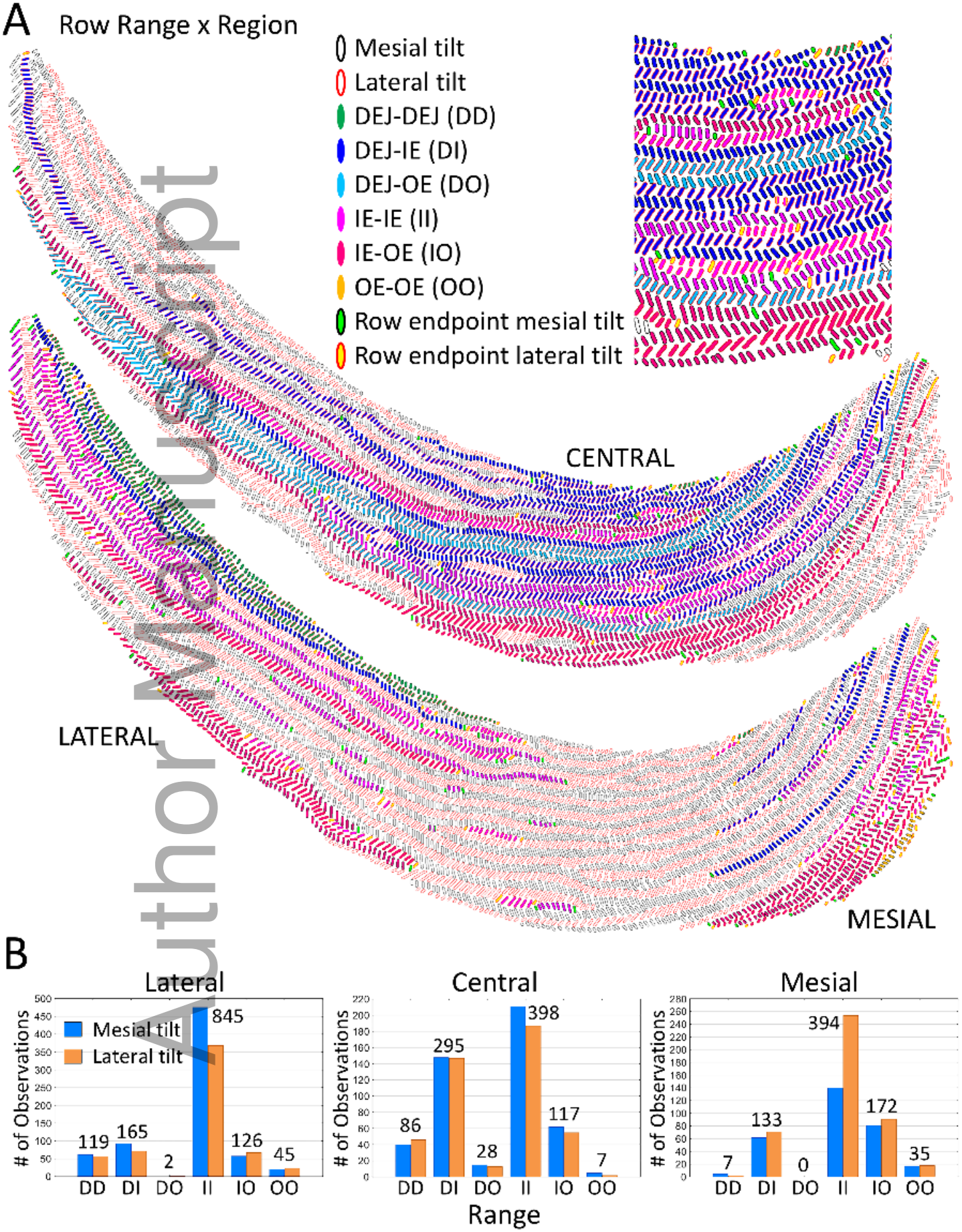

joa_13053_f5.tif

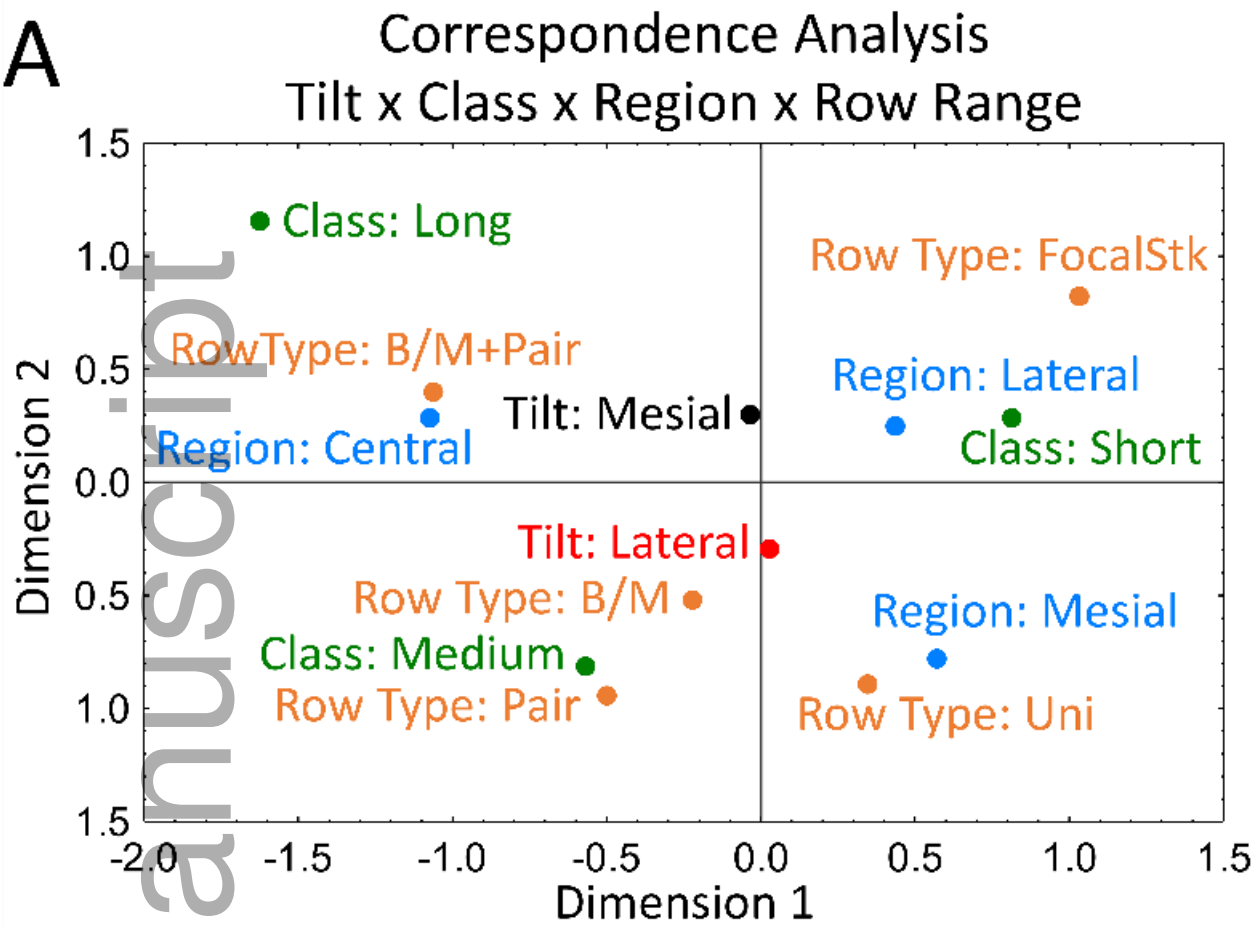

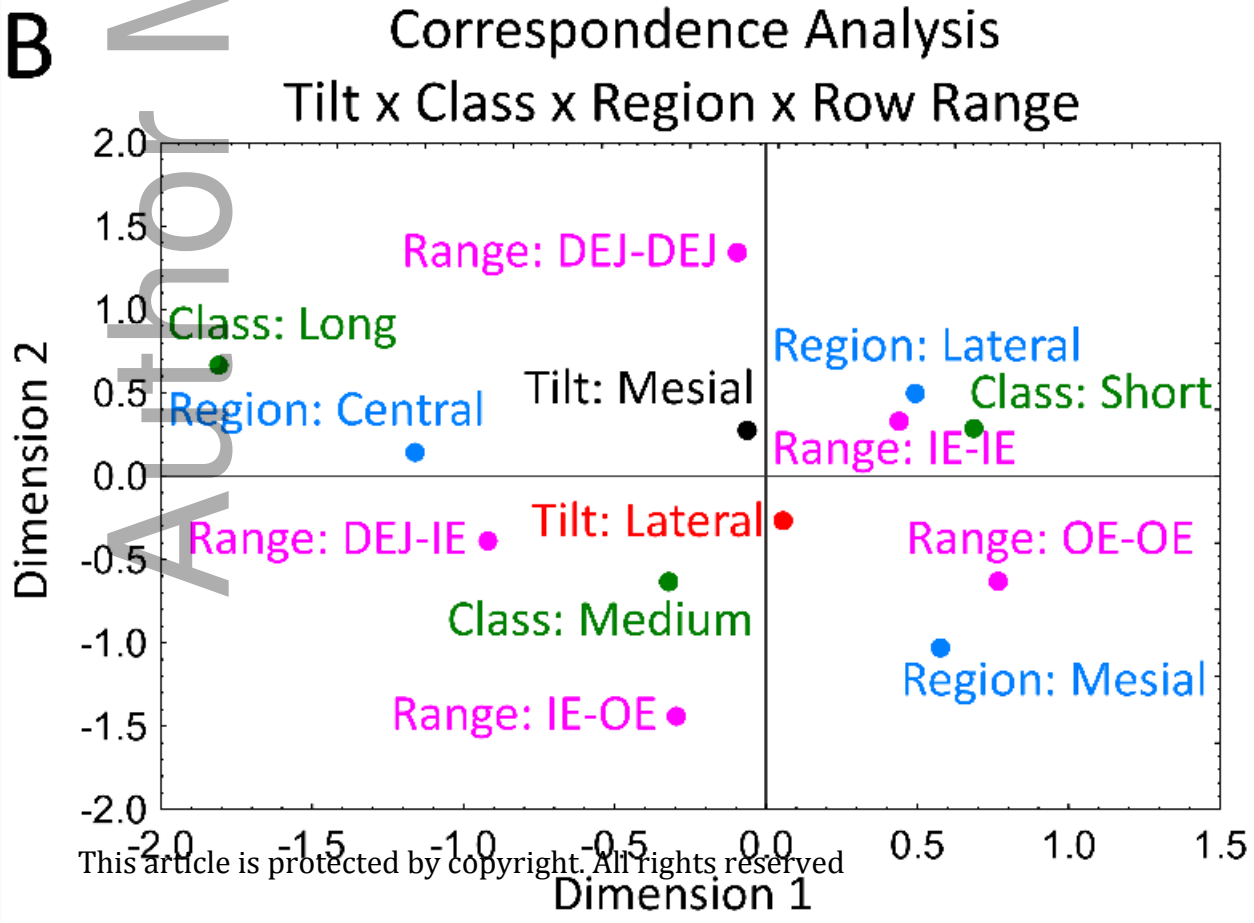

joa_13053_f6.tif

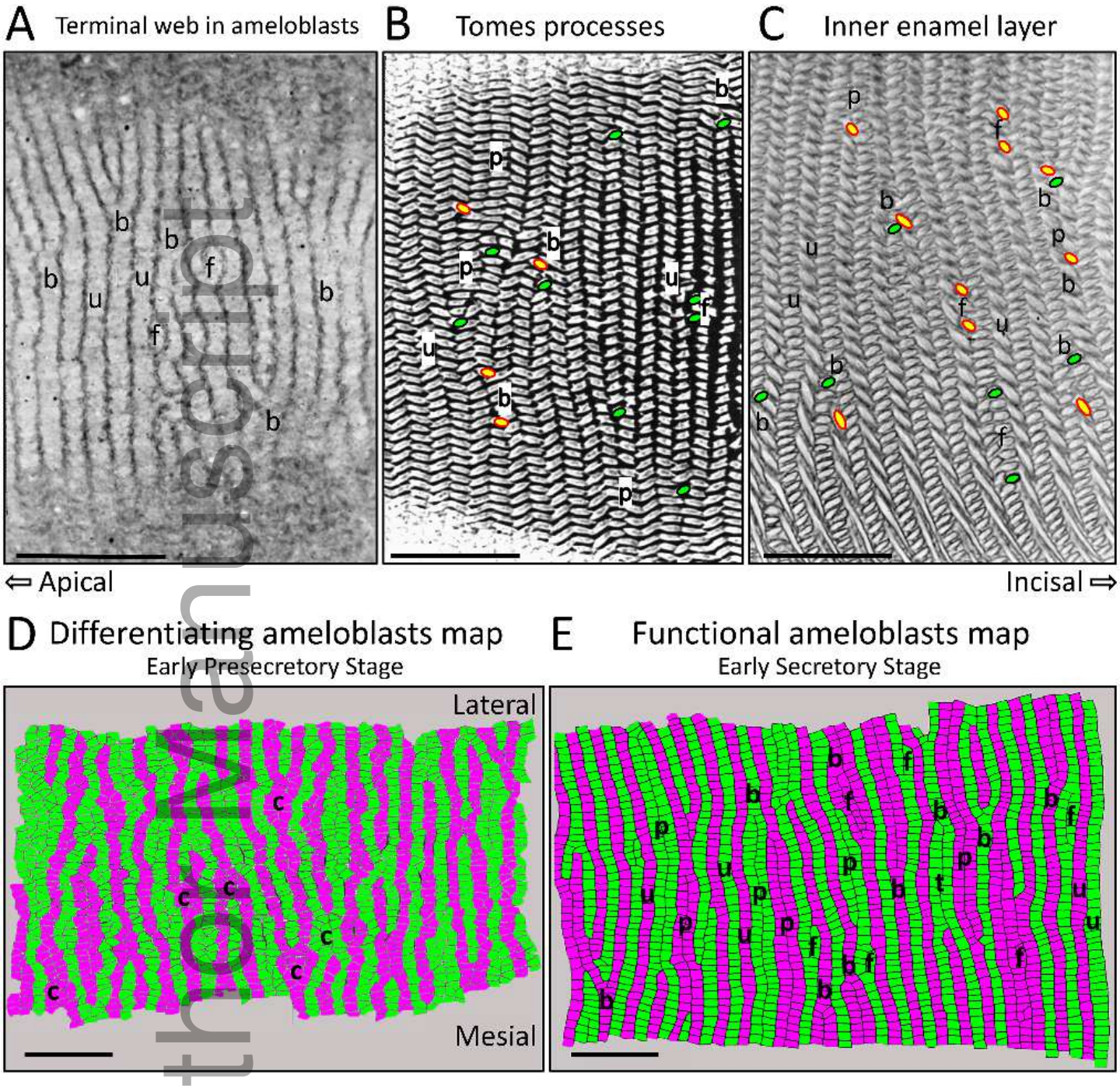

joa_13053_f7.tif

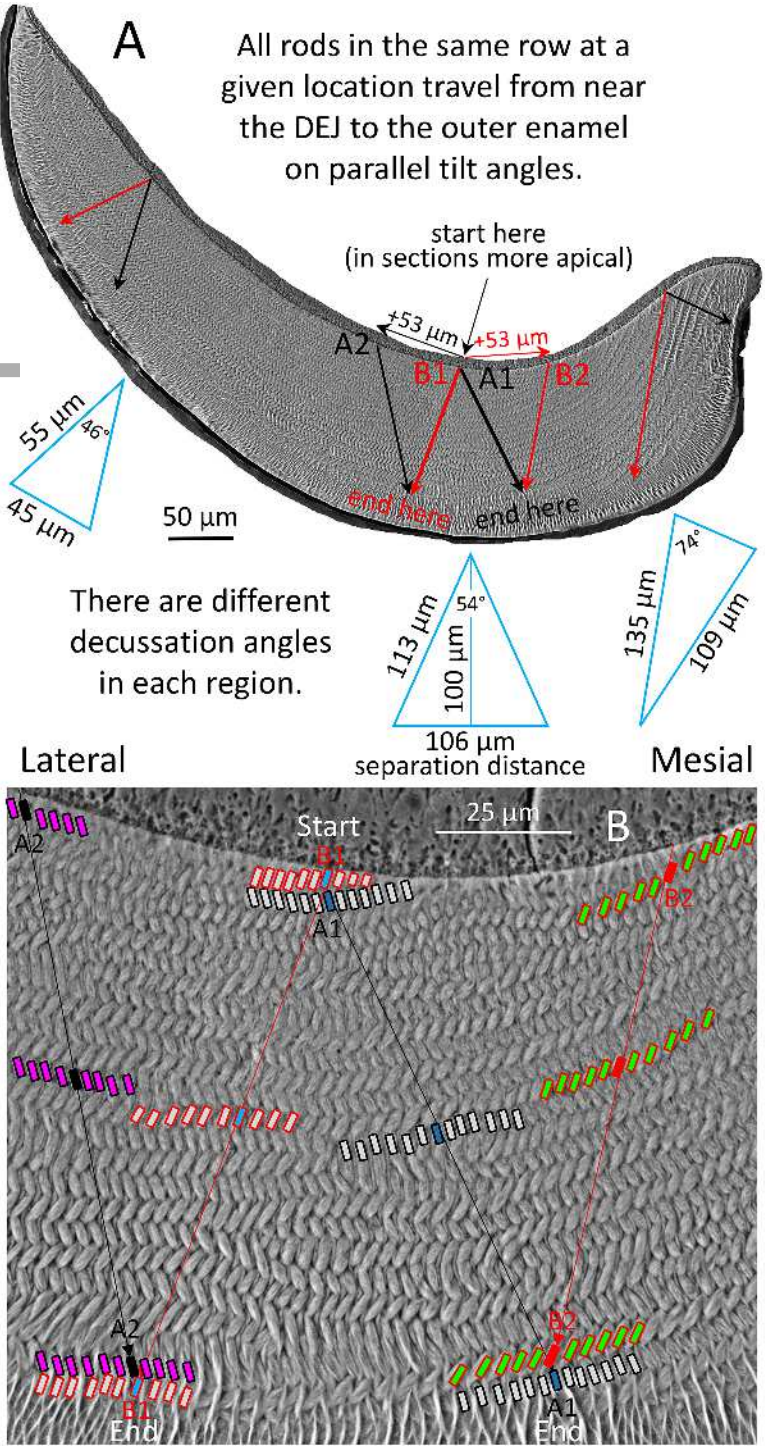

joa_13053_f8.tif